Acetylene Polymerization

International Edition: DOI: 10.1002/anie.201702685
German Edition: DOI: 10.1002/ange.201702685

Pressure-Induced Polymerization of Acetylene: Structure-Directed Stereoselectivity and a Possible Route to Graphane

Jiangman Sun[+], Xiao Dong[+], Yajie Wang, Kuo Li, Haiyan Zheng,* Lijuan Wang, George D. Cody, Christopher A. Tulk, Jamie J. Molaison, Xiaohuan Lin, Yufei Meng, Changqing Jin, and Ho-kwang Mao*

Abstract: *Geometric isomerism in polyacetylene is a basic concept in chemistry textbooks. Polymerization to cis-isomer is kinetically preferred at low temperature, not only in the classic catalytic reaction in solution but also, unexpectedly, in the crystalline phase when it is driven by external pressure without a catalyst. Until now, no perfect reaction route has been proposed for this pressure-induced polymerization. Using in situ neutron diffraction and meta-dynamic simulation, we discovered that under high pressure, acetylene molecules react along a specific crystallographic direction that is perpendicular to those previously proposed. Following this route produces a pure cis-isomer and more surprisingly, predicts that graphane is the final product. Experimentally, polycyclic polymers with a layered structure were identified in the recovered product by solid-state nuclear magnetic resonance and neutron pair distribution functions, which indicates the possibility of synthesizing graphane under high pressure.*

When unsaturated molecules are significantly compressed by external pressure, they tend to polymerize into extended structures. This is called pressure-induced polymerization (PIP). In a typical sequence, triple bonds polymerize into double bonds then single bonds, and carbon transforms from sp-hybridization to sp^2 and then sp^3. In the C/H system, many intriguing materials like graphane are predicted but were not stoichiometrically synthesized. PIP is considered an important method for this synthesis because the ratio of the elements can be sustained well under external pressure.

Acetylene (C_2H_2) is the simplest alkyne. It is used as building blocks for synthesizing larger molecules or materials like benzene and polyacetylene (PA). The ratio of C:H in acetylene is 1:1, equal to that in graphane, suggesting it is a reactant candidate. The PIP of acetylene has been studied by several groups as a prototype pressure-induced reaction.[1–5] At room temperature, acetylene polymerizes around 4.2 GPa without any catalyst.[4] With simultaneous laser irradiation, a more branched PA is produced.[5] At 77 K, acetylene polymerizes at ca. 11 GPa. The reaction is believed to be topochemically controlled and the product is mainly *cis*-PA.[6] Despite considerable spectroscopic and crystallographic research,[1,2,4,6,7] the stereoselectivity of producing *cis*-PA is still not understood and further reaction under higher pressures has not been explored. Here, we determined the crystal structure of acetylene under high pressure right before the PIP using in situ neutron diffraction and simulated the reaction process theoretically, based on which we explain the stereoselectivity in the PIP of crystalline acetylene. Following this proposed route predicts that graphane is the final product. To find experimental evidence, we synthesized various acetylene PIP products using Paris–Edinburgh cells (PE cells),[8,9] and examined their structures using solid-state nuclear magnetic resonance (ssNMR) and neutron pair distribution function (NPDF). We identified layered polycyclic polymers in the product and our research suggests the possibility of synthesizing graphane via the PIP of acetylene.

Acetylene adopts an orthorhombic structure from 1 to 5.7 GPa, as determined by in situ neutron diffraction. Upon further compression, the diffraction peaks disappear abruptly, indicating the collapse of the lattice and the polymerization of acetylene. The crystal structure of acetylene and the corresponding Rietveld refinement plot at 5.7 GPa is shown in Figure 1, and the crystallographic data are shown in Table S1 and S2 in the Supporting Information.

As anticipated, the length of the C≡C triple bond (1.172 Å) and C−D bond (1.025 Å) did not change significantly upon compression, while the intermolecular distances compressed.

The direction of the chain growth was predicted to be along the face diagonal of the *a*–*b* plane in the literature (gray line in Figure 1 a).[2] Chain elongation along the $a+b$ or $a-b$ direction is expected to result in *trans*-PA, while alternate growth along the $a+b$ and $a-b$ would form *cis*-PA. However,

[*] Dr. J. Sun,[+] Dr. X. Dong,[+] Dr. Y. Wang, Dr. K. Li, Dr. H. Zheng, Dr. L. Wang, Dr. X. Lin, Dr. Y. Meng, Dr. H.-k. Mao
Center for High Pressure Science and Technology Advanced Research
Beijing, 100094 (P.R. China)
E-mail: likuo@hpstar.ac.cn
zhenghy@hpstar.ac.cn
Dr. G. D. Cody, Dr. Y. Meng, Dr. H.-k. Mao
Geophysical Laboratory, Carnegie Institution of Washington
Washington, DC 20015 (USA)
Dr. H.-k. Mao
HPSynC, Geophysical Laboratory, Carnegie Institution of Washington
Argonne, IL 60439 (USA)
Dr. C. A. Tulk, J. J. Molaison
Neutron Sciences Directorate, Oak Ridge National Laboratory
Oak Ridge, TN 37830 (USA)
Dr. C. Jin
Institute of Physics, Chinese Academy of Sciences
Beijing, 100190 (China)
and
Collaborative Innovation Center of Quantum Matter
Beijing (China)
[+] These authors contributed equally to this work.
Supporting information and the ORCID identification number(s) for the author(s) of this article can be found under: https://doi.org/10.1002/anie.201702685.

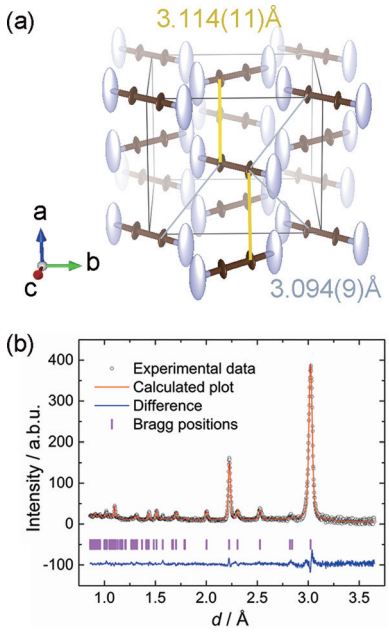

Figure 1. a) Crystal structure of acetylene at 5.7 GPa. The brown and light blue ellipsoids are carbon and deuterium atoms, respectively. The shortest distances between the carbon atoms in neighboring molecules are marked by yellow and gray solid lines. b) Rietveld refinement plot of C_2D_2 at 5.7 GPa. The black circles, red solid line, blue solid line and the violet bars are for the experimental data, simulated data, difference and Bragg positions, respectively.

there was no obvious explanation for the preference of *cis*-PA. After careful examination of the crystal structure and theoretical calculations mentioned below, we found that the nearest intermolecular C···C distance along the face diagonal of *a*–*c* plane is also around 3.1 Å, almost the same as the *a*–*b* plane. This indicates the possibility of a reaction on the *a*–*c* plane (yellow line in Figure 1 a). Furthermore, the displacement ellipsoid of carbon is extended on the *a*–*c* plane with its longest axis along the *c*-axis (restricted by the symmetry, it cannot point to the neighboring molecule on the *a*–*c* direction). The deuterium ellipsoid elongates along the *a*-axis and approximately point to the deuterium of the neighboring C_2D_2 on the *a*–*c* plane. These features indicate a stronger interaction between the neighboring molecules on the *a*–*c* plane. If the acetylene molecules react with their neighbors on the *a*–*c* plane, *cis*-PA will be obtained. Most importantly, regardless of whether the chain grows along the $a+c$/*a*–*c* direction or alternately along $a+c$ and *a*–*c*, the product will be *cis*-PA, which explains the *cis*-polymer production preference.

To have a direct view of the reaction process, how the crystalline acetylene polymerizes, and what the next reaction is, a metadynamic simulation was performed with the structural model of the molecular crystal C_2H_2 obtained experimentally. When the pressure was set at 10 GPa, the molecules randomly oriented first and then transformed to amorphous poly-acetylene (Figure 2 a). Both *trans*- and *cis*-PA sections were identified, together with a few 5- and 6-membered rings, which makes the structure amorphous and distorts the chains. When the pressure was set at 15 GPa, the lowest unoccupied molecular orbital (LUMO) of the acetylene molecules extended and overlapped their neighbors (Figure S1) and well-ordered *cis*-PA was produced (Figure 2 b). Two neighboring acetylene molecules rotated towards each other to bond and the two carbon atoms at the ends of the chain pointed to their neighboring molecules along the chain direction. The chains extended along the $a+c$ direction, in agreement with our crystal structure analysis. This simulation perfectly explains the stereoselectivity of *cis*-PA.

However, when the simulation continued the *cis*-PA phase surprisingly polymerized into a layered intermediate structure between a branched PA and graphane (Figure 2 b). Starting from the predicted *cis*-PA with a perfect lattice, every second carbon atom on one *cis*-PA chain bonds to one carbon atom on the neighboring chain on one side. Thus, six-membered rings are formed between the two chains with three members from each chain. The other half of the non-bonded carbon atoms turn to the chain on the other side and bond in a similar way. Therefore, the chains are zipped together to form a sheet and the product is perfect graphane (Figure 2 c).[10]

To investigate the process experimentally, in situ IR spectra up to 27 GPa were measured using a diamond anvil cell (DAC). *Trans*- and *cis*-C=C and saturated C–C single bonds were identified (Figure S2, details in the Supporting Information), in agreement with the literature.[4] To obtain structural details, we used a Paris–Edinburgh cell to synthesize the sample on a milligram scale. Compared to DAC experiments, the thermal or photo effect generated by the laser or other detection methods can be completely precluded in this method, so the reaction was solely induced by the pressure.

Sample P1 was synthesized at 5 GPa as brown powder. Its infrared spectrum is shown in Figure 3. Compared to the DAC product, the most distinctive features are the strong peaks at 1127 cm^{-1} and 1336 cm^{-1} that correspond to the skeleton stretching ($\nu_{skeleton}$) and CH in-plane deformation of the *cis*-C=C, respectively ($\beta_{CH,c}$).[4,11] In addition, the CH stretching mode ($\nu_{CH,c}$, 3050 cm^{-1}) is higher than the corresponding mode in the DAC sample (3013 cm^{-1}, *trans*-C=C, $\nu_{CH,t}$).[4,11] All of these factors indicate the dominating content of *cis*-PA in P1. The peaks between the 912 cm^{-1} and 1065 cm^{-1} are attributed to the C–H out-of-plane deformation in *trans*-CH=CH- ($\gamma_{CH,t}$), or in -(*trans* CH=CH)$_m$- ($m=1, 2$) between -(*cis* CH=CH)- ($\gamma_{CH,tinc}$), which suggests the existence of *trans*-PA. Peaks related to the C–H stretching mode ($\nu_{CH,s}$) and C–C stretching mode ($\nu_{C-C,s}$)/CH_2 deformation mode ($\delta_{CH,s}$) of saturated carbon were observed at 2934 cm^{-1} and 821 cm^{-1} respectively, which are evidence of sp^3 carbon. Thus, we can conclude that P1 is a branched PA, with *cis*-PA dominating. This is consistent with the neutron diffraction and theoretical calculation predictions. It is well known that *cis*-PA is not thermodynamically favored. During polymerization in solution at ambient pressure, *cis*-PA is kinetically favored due to the stereochemistry of the catalyst. Here, our sample P1 obtained at high-pressure conditions also produced *cis*-PA as the main product without a catalyst.

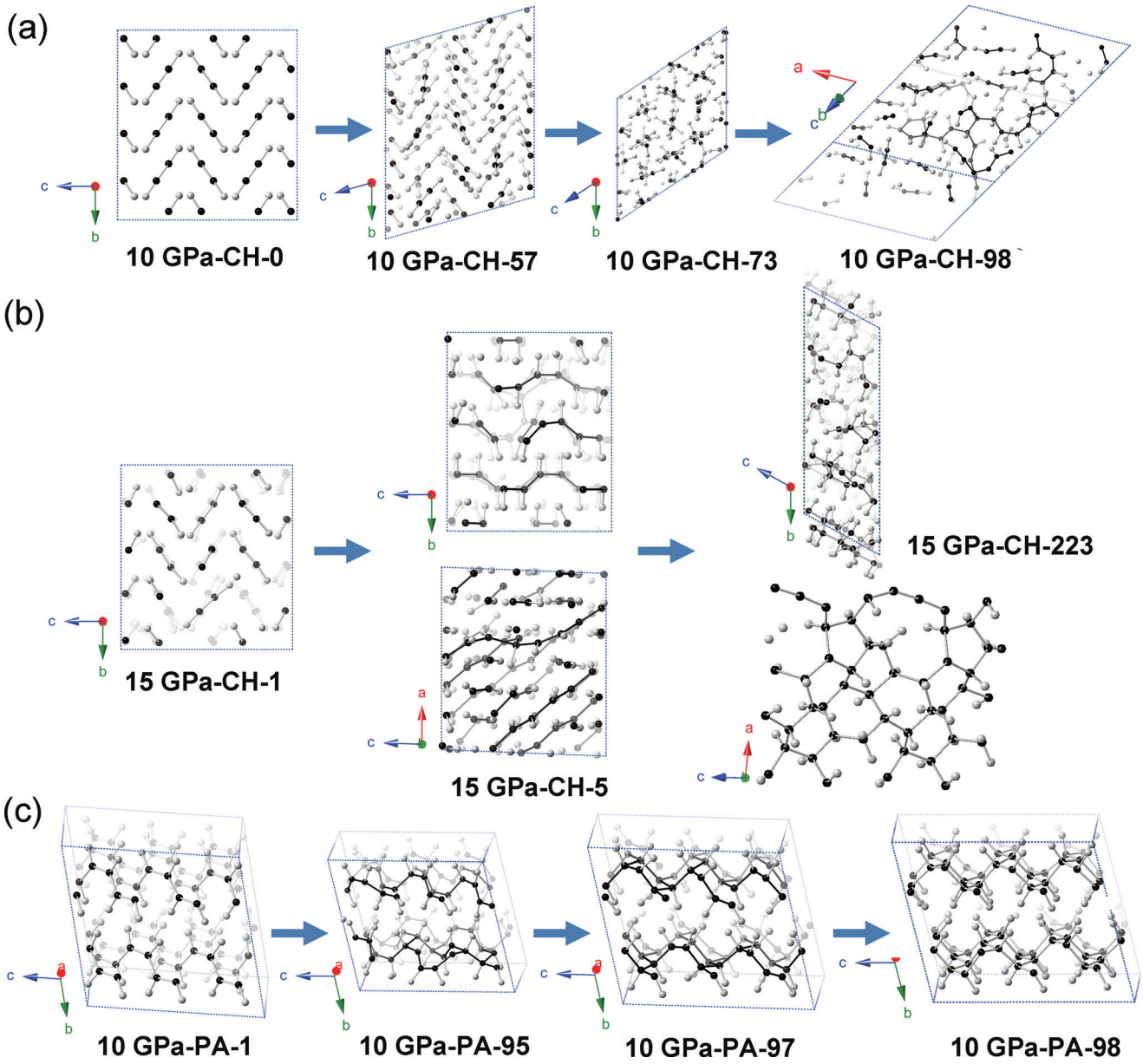

Figure 2. Selected structure models of metadynamic simulations. a) 10 GPa, b) 15 GPa, and c) 10 GPa from *cis*-PA theoretically predicted by PIP. CH and PA represent that the starting materials are crystalline C_2H_2 and *cis*-PA, respectively. The numbers following CH and PA are the generation numbers.

When the applied pressure was increased (10 GPa), we obtained yellow powder (P2) with a C:H molar ratio of 1:1 according to the elemental analysis. Its IR spectrum looks very similar to the sample synthesized by DAC (Figure 3). Compared with P1, the signal of the saturated C–H bond was enhanced, while the *cis*-PA signal disappeared, suggesting that the *cis*-C=C bonds had reacted. Similar features were reported for the sample compressed in a DAC with laser irradiation, which was recognized as a highly branched polymer (more saturated).[5] Therefore, P2 should be a more saturated C:H compound due to a higher degree of polymerization.

To understand the local structure of P2, solid-state ^{13}C and ^{1}H NMR spectra were measured and showed that P2 still contained PA but with a significant amount of sp^3 carbon (Figure 4a and S3). In the ^{13}C cross-polarization magic-angle-spinning solid-state NMR (^{13}C CPMAS ssNMR) spectrum, the peaks at 129.5 ppm and 134.7 ppm are reasonably assigned to the carbon in *cis*-PA and *trans*-PA, respectively (Figure 4a).[13] The content of the *trans*-PA is higher than the *cis*-PA and consistent with the IR result shown above. The next most prominent peak centered at 46.1 ppm is in the region of sp^3 carbon and is attributed to the -CH- tertiary carbon (methine) in $RCH(-CR{=}CR_2)_2$ group, which is solid evidence of cross-linked PA. The formation of methine carbon and subsequent cross-linking likely occurs through pressure-induced cycloaddition reactions between the PA, which implies ring structures formed. The domination of

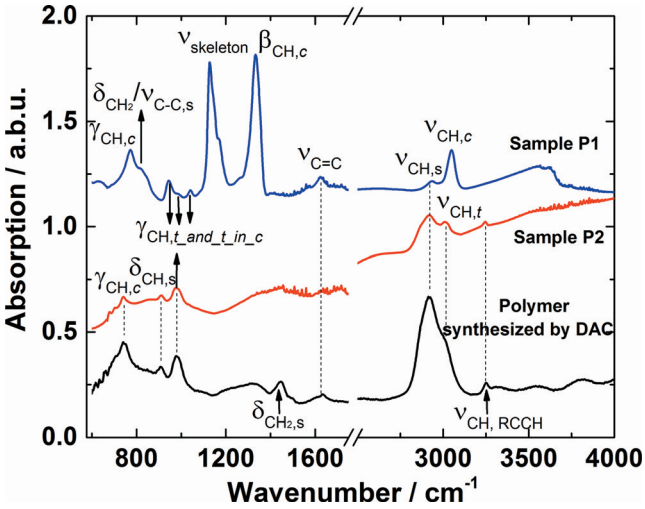

Figure 3. Infrared spectra of sample P1, P2, and the sample synthesized by DAC. The vibration modes are assigned according to the literature[4,11,12] and the IR modes abbreviations are as follows: *anti*-symmetric stretching of C–H in acetylene ($\nu_{CH,RCCH}$), stretching of C–H in *cis*-PA, *trans*-PA and saturated molecule($\nu_{CH,c}$, $\nu_{CH,t}$, $\nu_{CH,s}$), stretching of C=C, C–C and skeleton ($\nu_{C=C}$, $\nu_{C-C,s}$, $\nu_{skeleton}$); deformation of CH_2 and C–H in saturated molecule ($\delta_{CH2,s}$, $\delta_{CH,s}$), in-plane and out-of-plane deformation of C–H in *cis*-C=C ($\beta_{CH,c}$, $\gamma_{CH,c}$), out-of-plane deformation of C–H in *trans*-C=C ($\gamma_{CH,t}$), or -(*trans* CH=CH)$_m$- ($m=1$, 2) between -(*cis* CH=CH)$_n$- ($\gamma_{CH,t\ in\ c}$).

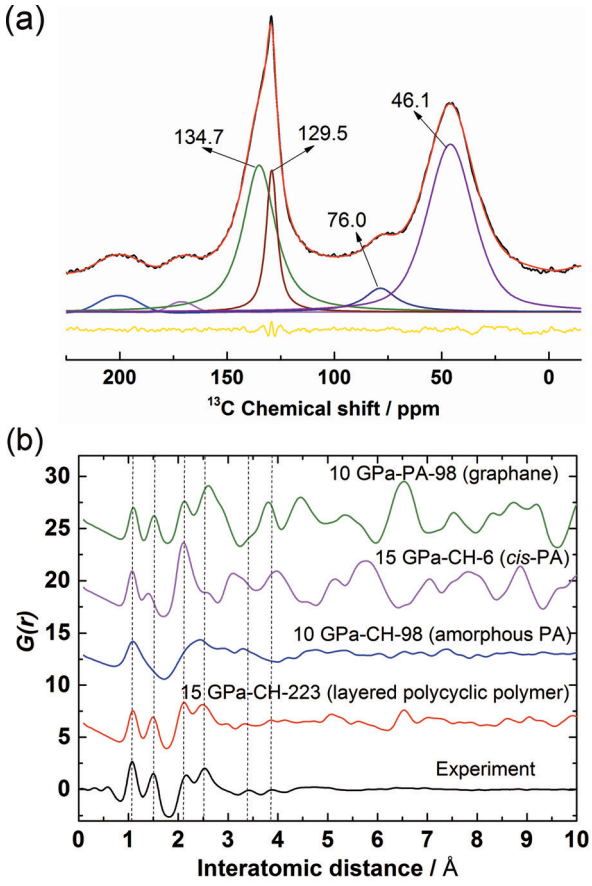

Figure 4. a) ^{13}C cross-polarization (^1H-^{13}C) magic-angle-spinning solid-state NMR spectrum (^{13}C CPMAS ssNMR) of sample P2. The black, red and yellow lines represent the experimental results, the cumulative fit peak, and regular residual, respectively. The peak at 76 ppm is in the region of C≡C. b) The neutron PDF experiment data of deuterated sample P2 (P2-D) and the modeled PDFs $G(r)$ of selected structural models of the metadynamic simulations shown in Figure 2. The CH and PA represent that the starting material are crystalline C_2H_2 and *cis*-PA, respectively. The following numbers are the generation numbers.

trans-PA indicates that under higher pressure, most of the *cis*-PA transferred into sp^3 carbon species.

The significant presence of a ring structure in sample P2 is solidly confirmed by the neutron PDF of the deuterated sample. We simulated the $G(r)$ patterns using the structural models obtained from the metadynamic simulation (Figure 2). The results (Figure 4b) indicate that P2 is similar to the model of a layered polycyclic structure (Figure 2b). Other models including amorphous PA (Figure 2a), *cis*-PA (Figure 2b), and graphane (Figure 2c) do not match the PDF data. The observed first C–C distance is 1.5 Å corresponding to the C–C single bond, which means sp^3 carbon dominates in P2. As shown in Figure 2b, these sp^3 carbons are mainly present in cyclic structures. Based on the structures of P1 and P2, we conclude that our experimental results satisfactorily confirm the reaction route shown in Figure 2b. The acetylene polymerizes into *cis*-PA first (P1), then transforms into a layered structure with dominant sp^3 carbon (P2). It is worthy to mention that the sample may decompose to form graphite when the gasket was not perfectly sealed, which is another topic and will not be discussed here.

From these investigations, we can understand the PIP process of acetylene. In the first step, it polymerizes into PA and in the second step, PA polymerizes into a saturated layered structure with ring components. Two key factors control the PIP process. The first is the crystal structure of acetylene, which guides the polymerization along the $a+c$/a–c direction under pressure and forms *cis*-PA. The second is the thermal effect, which perturbs the ordering and generates an amorphous structure. Compressing the crystalline PIP *cis*-PA is expected to generate graphane, but the random cross-links in PA will destroy or disturb the ordering. This is why crystalline graphane was not obtained by PIP of acetylene at room temperature. Following theoretical calculations, compression under low temperature will reduce the thermal effect[6] and facilitates a structure-directed reaction, allowing graphane to be obtained.

In summary, we determined the crystal structure of acetylene under high pressure by in situ neutron diffraction. Consequently, the reaction route of acetylene was solved and the *cis*-PA domination was understood. The PIP of acetylene is a potential route for the synthesis of graphane and a polycyclic polymer with layered structure was observed in our experiment. This polymer can be recognized as an intermediate between PA and graphane. Based on this research, we predict that compression under low temperature would facilitate the production of graphane. Our research uncovers the reason for stereoselectivity in the PIP of acetylene and provides important recommendations for the synthesis of graphane.

Experimental Section

High purity d_2-acetylene (99% D atom) was used for the in situ neutron diffraction measurements without purification. The experiment was carried out at Spallation Neutrons and Pressure Diffractometer (SNAP), Spallation Neutron Source (SNS), Oak Ridge National Lab (ORNL). Acetylene of 99% purity was purified by passing it through a $NaHSO_3$ aqueous solution and a cold trap (−78 °C) to remove acetone, followed by drying it over fine granular calcium chloride.[4] A DAC equipped with type IIa diamonds was used to apply pressure for in situ IR measurements. The purified acetylene gas was condensed in the DAC and sealed quickly under the liquid nitrogen temperature. Then, the DAC was warmed to room temperature. The high-pressure in situ IR spectra were collected on a Bruker VERTEX 70v FTIR spectrometer and a custom IR microscope. The samples P1, P2, and P2-deuterated were synthesized by the VX3 PE cell with tungsten carbide anvils. The P2-deuterated sample was used for the neutron PDF measurements. Details of the in situ neutron diffraction and in situ IR of C_2H_2, high-pressure synthesis of the sample P1, P2 and P2-deuterated, ssNMR measurement, and neutron PDF of the recovered samples and metadynamic calculations are given in the Supporting Information.

Acknowledgements

The authors acknowledge the support of NSAF (Grant No:U1530402) and National Natural Science Foundation of China (NSFC) (Grant No: 21501162 and 21601007). The research at Oak Ridge National Lab's Spallation Neutron Source was sponsored by the Scientific User Facilities Division, Office of Basic Energy Sciences, U.S. Department of Energy.

Conflict of interest

The authors declare no conflict of interest.

Keywords: acetylene · graphane · neutron diffraction · pressure-induced polymerization · solid-state reactions

How to cite: *Angew. Chem. Int. Ed.* **2017**, *56*, 6553–6557
Angew. Chem. **2017**, *129*, 6653–6657

[1] R. LeSar, *J. Chem. Phys.* **1987**, *86*, 1485–1490.
[2] K. Aoki, S. Usuba, M. Yoshida, Y. Kakudate, K. Tanaka, S. Fujiwara, *J. Chem. Phys.* **1988**, *89*, 529–534.
[3] K. Aoki, Y. Kakudate, S. Usuba, M. Yoshida, K. Tanaka, S. Fujiwara, *J. Chem. Phys.* **1988**, *88*, 4565–4568.
[4] M. Sakashita, H. Yamawaki, K. Aoki, *J. Phys. Chem.* **1996**, *100*, 9943–9947.
[5] M. Ceppatelli, M. Santoro, R. Bini, V. Schettino, *J. Chem. Phys.* **2000**, *113*, 5991–6000.
[6] C. C. Trout, J. V. Badding, *J. Phys. Chem. A* **2000**, *104*, 8142–8145.
[7] K. Aoki, Y. Kakudate, M. Yoshida, S. Usuba, K. Tanaka, S. Fujiwara, *Synth. Met.* **1989**, *28*, D91–D98.
[8] J. M. Besson, R. J. Nelmes, G. Hamel, J. S. Loveday, G. Weill, S. Hull, *Phys. B* **1992**, *180*, 907–910.
[9] S. Klotz, G. Hamel, J. Frelat, *High Pressure Res.* **2004**, *24*, 219–223.
[10] X.-D. Wen, L. Hand, V. Labet, T. Yang, R. Hoffmann, N. W. Ashcroft, A. R. Oganov, A. O. Lyakhov, *Proc. Natl. Acad. Sci. USA* **2011**, *108*, 6833–6837.
[11] M. Gussoni, C. Castiglioni, M. Miragoli, G. Lugli, G. Zerbi, *Spectrochim. Acta Part A* **1985**, *41*, 371–380.
[12] H. Shirakawa, S. Ikeda, *Polym. J.* **1971**, *2*, 231–244.
[13] H. W. Gibson, J. M. Pochan, S. Kaplan, *J. Am. Chem. Soc.* **1981**, *103*, 4619–4620.

Manuscript received: March 14, 2017
Version of record online: May 2, 2017

